Microbiology, Metabolites and Biotechnology
Journal home page:
MMB The former ARMMT

In Silico Pharmacokinetic Profiling, Molecular Docking, and Antioxidant Assessment of *Bis*-Urea Derivatives Derived from the Sorafenib Scaffold

Sajede Shoja[1]*, Elham Gholibegloo[1], Nosrat O (Allah) Mahmoodi[2]*

[1] *Department of Chemical Technologies, Iranian Research Organization for Science and Technology (IROST), PO Box 33535111, Tehran, Iran.*
[2] *Department of Medicinal Organic Chemistry, Faculty of Chemistry, University of Guilan, PO Box 41335-1914, Rasht, Iran.*

Article Info

Document Type:
Review Paper

Received 12/02/2026
Received in revised form 29/03/2026
Accepted 13/05/2026

Published 18/07/2026

Keywords:
Sorafenib
bis-Urea
Molecular Docking
Pharmacokinetic
ADME
Antioxidant

Abstract

Sorafenib, also known as Nexavar, is a multikinase inhibitor with a diarylurea scaffold. The Food and Drug Administration approved it for the treatment of advanced hepatocellular and renal cell carcinoma. Its well-defined structural framework has served as a template for the development of numerous analogs designed to enhance pharmacological efficacy and minimize adverse effects. In this work, seven previously synthesized bis-urea derivatives, for which cytotoxicity (MTT), antibacterial activity, and initial in silico studies have been reported, were further evaluated using molecular docking, in silico ADME studies, and antioxidant assay. These compounds combined diverse linker moieties, enabling structural variations that could modify receptor binding and pharmacokinetic performance. Molecular docking studies of the compounds in complex with selected target receptors, using sorafenib as the positive control, indicated that some derivatives revealed comparable or improved predicted hydrogen bond interactions and binding affinities relative to sorafenib. These results reflect computational predictions of ligand–receptor interactions. Pharmacokinetic evaluations were conducted using in silico ADME (Absorption, Distribution, Metabolism, and Excretion) to supplement the docking data. These analyses demonstrated promising characteristics for the target compounds, accompanied by acceptable pharmacological properties, such as balanced lipophilicity, oral bioavailability, and favorable metabolic stability, thus supporting their suitability for further biological assessment. In addition, all compounds were evaluated for their antioxidant activities using standard DPPH assays. Some derivatives showed notable antioxidant effects compared to ascorbic acid as the standard. Pharmacokinetic aspects were evaluated in silico to complement docking studies, while antioxidant activity was explored as an additional physicochemical feature rather than a primary mechanism associated with kinase inhibition.

1. Introduction

Urea-based scaffolds have been used for some time to make new medicines (Li *et al.,* 2005; Terefenko *et al.,* 2005). These scaffolds can interact with various biological targets through multiple non-covalent interactions. (Guan *et al.,* 2014). Their biological relevance is largely attributed to the presence of NH functional groups, because the groups help form bonds with amino acids in the proteins they target, such as hydrogen bonds. This affects how well these interactions significantly influence binding affinity and target selectivity. (Lim *et al.,* 2009; Stumpe & Grubmüller, 2007).

Tumor cell proliferation, angiogenesis, and apoptosis are key biological processes that together drive tumor growth and metastasis. These processes, including uncontrolled cell division, formation of new blood vessels, and programmed cell death, are regulated by distinct proteins and signaling pathways (Lemmon & Schlessinger, 2010; Liao, 2007; Winum *et al.,* 2012; Zhang *et al.,* 2018). The main signaling pathway that goes from the cell membrane to the nucleus is the Ras-mitogen-activated protein kinase signaling pathway, also known as the MAPK pathway, which includes the Ras/Raf/MEK/ERK signal transduction cascade. Raf is a serine/threonine kinase that consists of three isoforms: A-Raf, B-Raf, and Raf-1 or c-Raf. Blocking the Raf/MEK/ERK pathway at the level of Raf kinases can effectively prevent tumors driven by this pathway (Davies *et al.,* 2002; Dumaz & Marais, 2003; Holderfield *et al.,* 2013).

B-Raf mutations are among the most common oncogenic modifications in cancers, frequently observed in malignant melanomas as well as thyroid, lung, ovarian, and liver cancers (Nazarian *et al.,* 2010; Yuen *et al.,* 2002). Thus, B-Raf has been identified as a critical target for the design and synthesis of anticancer agents. Furthermore, multikinase inhibition targeting B-Raf, B-RafV600E, and VEGFR-2 represents a hopeful method for cancer therapy.

*Corresponding authors E-mail: sajede.shoja@irost.ir; nosmahmoodi@gmail.com
DOI: 10.22104/mmb.2026.8141.1198
https://mmb.irost.ir/article_1713.html

Sorafenib, a diarylurea-containing multikinase inhibitor, has received FDA approval for the treatment of advanced hepatocellular carcinoma due to its pronounced antiproliferative effects (*Nexavar® (Sorafenib) Scientific Discussion EMEA WC500027707.*, 2007; *Sorafenib, BAY43-9006 (Nexavar®, Bayer) NDA 21923 Medical Review* 2005).

Mechanistically, sorafenib disrupts the Raf/MEK/ERK signaling cascade by inhibiting Raf kinases. It simultaneously targets additional kinases associated with tumor angiogenesis and progression, including PDGFR, VEGFR-2, c-KIT, and FLT-3 (Wilhelm *et al.,* 2008). Its therapeutic efficacy in oncology is supported by this broad-spectrum inhibition.

The preliminary in silico, cytotoxic (MTT), and antibacterial evaluations of these bis-urea derivatives have been reported previously (Shoja *et al.,* 2020). The present work does not aim to reproduce those findings, but rather to provide a focused and extended computational investigation of ligand–receptor interactions through molecular docking, together with in silico pharmacokinetic (ADME) analyses and complementary antioxidant evaluation. Each compound incorporates a distinct linker moiety, strategically designed to modulate intermolecular interactions and improve receptor selectivity. Therefore, in this study, pharmacokinetic profiling and molecular docking analyses were employed to explore the interaction patterns and drug-likeness of the synthesized bis-urea derivatives, without drawing definitive conclusions about their biological efficacy.

2. Materials and Methods

Based on modifications of the sorafenib structure, seven previously synthesized *bis*-urea derivatives 1a-g were evaluated for their biological potential, including molecular docking studies, pharmacokinetic analyses, and antioxidant assays (Figure 1). It is necessary to explain that compounds 1a–1g in the present study correspond to compounds labeled as 3a–3g reported in our previous work (Shoja *et al.,* 2020); the numbering was adjusted for clarity within the present study.

2.1. Receptor Structure Selection and Preparation for Molecular Docking

Sorafenib has ten receptors with particular pharmacological actions, including BRAF (Uniprot ID: P15056), RAF1 (Uniprot ID: P04049), VEGFR2 (Uniprot ID: P35968), PDGFRB (Uniprot ID: P09619), FGFR1 (Uniprot ID: P11362), KIT (Uniprot ID: P10721), RET (Uniprot ID: P07949), FLT1 (Uniprot ID: P17948), FLT3 (Uniprot ID: P36888), and FLT4 (Uniprot ID: P35916) (*https://www.drugbank.ca/drugs/DB00398*). Suitable templates, which have a high degree of sequence similarity with the aforementioned targets, were identified using BLASTp (*https://blast.ncbi.nlm.nih.gov/Blast.cgi*). Some of these proteins were found to have similar structures after first blasting their sequences and then searching for templates in the Protein Data Bank (PDB), including BRAF and RAF1 (PDB ID: 4RZV), FLT1, FLT3, and FLT4 (PDB ID: 5X02), and KIT and PDGFRB (PDB ID: 4HVS). Additionally, models selected from the PDB database for VEGFR2, FGFR1, and RET were 4ASD, 5A46, and 4CKJ, respectively.

BLASTp analysis was employed solely to identify homologous protein sequences and suitable crystallographic templates with high sequence coverage and identity. Structural similarity was inferred only after selecting experimentally resolved kinase domains from the Protein Data Bank (PDB) and was not assumed based on sequence alignment alone. Each receptor was docked independently using its own validated three-dimensional structure, and no generalization of docking results across different kinases was intended. Next, six candidate targets were prioritized for further molecular docking investigations. These six kinases were selected based on the availability of high-resolution crystallographic structures, presence of sorafenib-bound or ATP-binding kinase domains, and relevance to sorafenib's documented inhibitory profile. Other reported targets were excluded due to a lack of suitable structural data for reliable docking.

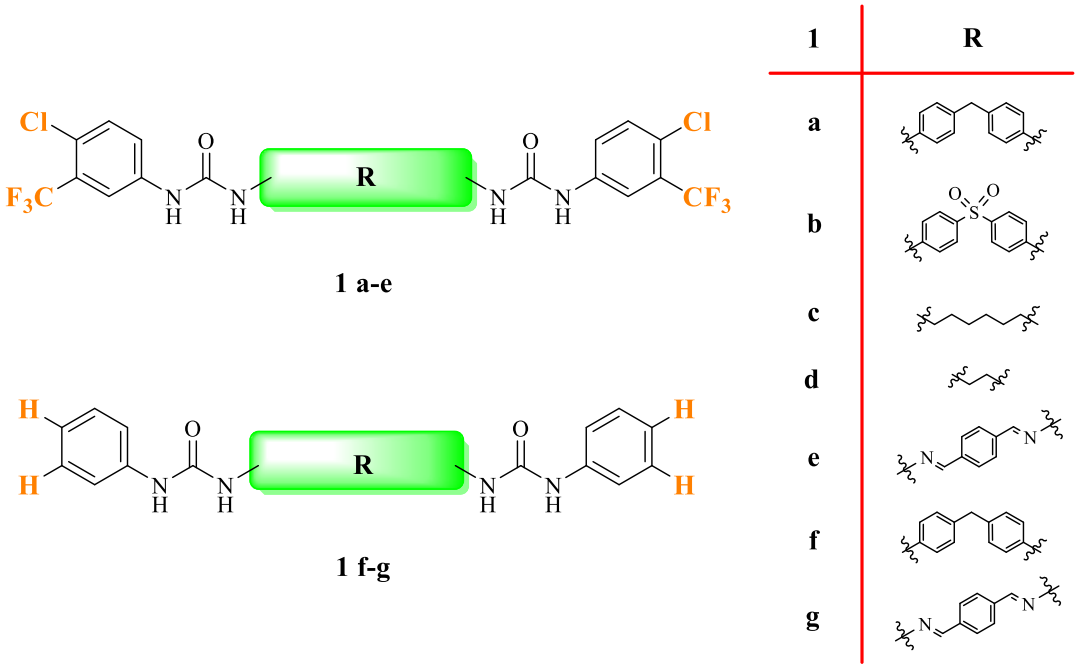

Figure 1. Structures of Bis-urea Derivatives, 1a-g

The final models were constructed following energy minimization using Swiss-PdbViewer DeepView version 4.1.0 (Guex & Peitsch, 1997). Model structures were validated through RAMPAGE (Lovell *et al.,* 2003) and ProSA servers (Sippl, 1993; Wiederstein & Sippl, 2007). Finally, 3-D models were visualized by AutoDock 4.2.6 (Morris *et al.,* 2009).

2.2. Molecular Docking

Molecular docking analyses were performed using AutoDock 4.2.6. Docking simulations were conducted at the ATP-binding sites of six selected kinases using sorafenib and its derivatives (1a–1g). All ligands were energy-minimized using HyperChem Professional version 8.0.8 prior to docking to obtain stable three-dimensional conformations. For VEGFR-2, the crystallographic structure co-crystallized with sorafenib (PDB ID: 4ASD) was employed as a positive control, and the active-site coordinates were defined based on the binding mode of sorafenib in this structure. For the remaining receptors, active-site regions were identified according to reported crystallographic ligand–receptor interactions. Grid boxes were centered on the ATP-binding pockets of each kinase. A relatively large grid box (100 × 100 × 100 points) with a spacing of 0.375 Å was applied to fully encompass the ATP-binding site and adjacent regions; however, because the grids were centered on the known active sites, a targeted docking strategy was employed rather than blind docking. Docking calculations were performed using the genetic algorithm (GA), with 10 GA runs, a population size of 150, a maximum of 2,500,000 energy evaluations, and 27,000 generations. For each ligand–receptor complex, the best binding pose was selected based on the lowest binding energy and favorable hydrogen-bond interactions within the dominant cluster. The binding affinities of the studied compounds were subsequently evaluated and compared with those of sorafenib.

2.3. Pharmacokinetic properties

ADME (absorption, distribution, metabolism, and excretion) properties of the synthesized compounds 1a–g were evaluated using QikProp (*QikProp, Schrödinger, LLC, New York, NY, 2018.* , 2018). The predicted parameters were as follows: QpLogPo/w (Predicted octanol/water partition coefficient logp), QP LogHERG (Predicted IC_{50} values for blockage of HERG K^+ channels), QPPCaco (Predicted Caco-2 cell permeability), QPlogKp (Predicted skin permeability), QpLogKHsa (Predicted binding to human serum albumin), percentage of human oral absorption, QpLogBB (Predicted brain/blood partition coefficient), and QPPMDCK (Predicted apparent MDCK cell permeability).

QPlogBB and QPPMDCK are indicators of blood–brain barrier penetration, where QPlogBB predicts the polarity of CNS drugs required to cross the barrier, and QPPMDCK estimates MDCK cell permeability, serving as a reliable mimic of the blood–brain barrier. The percentage of Human Oral Absorption is based on a quantitative multiple linear regression model that usually associates well with Human Oral Absorption, as both assess the same feature. Moreover, as a crucial fact for designing the drug, Lipinski's Rule of Five and Jorgensen's Rule of Three were calculated for each compound. The Lipinski's rule of five refers to mol_MW < 500, QPlogPo/w < 5, donorHB ≤ 5, accptHB ≤ 10. Compounds that comply with these limits are considered drug-like (the "five" means limits that are multiples of 5). Jorgensen's Rule of Three includes: QPlogS > -5.7, QP PCaco > 22 nm/s, and Primary Metabolites < 7. Molecules with fewer, and preferably no, violations of these rules are more likely to be considered as orally available compounds (Jorgensen & Duffy, 2000; Lipinski *et al.,* 2012).

2.4. DPPH radical-scavenging activity

DPPH radical-scavenging activities of compounds 1a-g were assessed, consistent with the literature (Jin *et al.,* 2012). To give a concentration of 6.25×10^{-5} M, the 2,2-diphenyl-2-picrylhydrazyl (DPPH) solution was prepared by dissolving an appropriate amount of DPPH in MeOH. Then, 3.9 mL of this solution was added to 0.1 mL of the sample solution in different concentrations (2000, 1000, 500, 250, 125, 62.5 µg/mL in MeOH). The samples were shaken vigorously and kept in the dark for 30 min, and then the decrease in the absorbance of the resulting solution was measured at 517 nm. MeOH was used as a blank, and a sample of 3.9 mL DPPH containing 0.1 mL of MeOH instead of the sample was used as a control.

Inhibition of free radical DPPH in percentage was calculated as Eq. (1):

$$\text{Radical scavenging activity} = \left(\frac{A_{blank} - A_{sample}}{A_{blank}}\right) \times 100 \qquad (1)$$

where A_{blank} is the absorbance of the negative control (including all reagents except test compounds), and A_{sample} is the absorbance of the test compounds. The antioxidant activity was measured with reference to the standard ascorbic acid absorbance values.

3. Results and Discussion

3.1. Chemistry

A set of seven bis-urea derivatives (1a–g, Figure 1 (Shoja *et al.,* 2020)) previously designed and synthesized based on modifications of the sorafenib structure and our interest in two-directional synthesis strategies with pharmacological relevance (Aliabadi *et al.,* 2018; Mahmoodi, Khalili, *et al.,* 2016; Mahmoodi, Namroudi, *et al.,* 2016; Mahmoodi *et al.,* 2014; Mahmoodi *et al.,* 2015). In the present work, with a constant focus on exploring useful compounds with therapeutic benefits, these synthesized bis-urea derivatives were evaluated for their biological potential, including molecular docking studies, pharmacokinetic analyses, and antioxidant assays.

3.2. Biology

3.2.1. Docking results of sorafenib and its derivatives (1a-g) in complex with candidate receptors

Docking results revealed differential binding affinities of sorafenib and its bis-urea derivatives toward the six selected kinases. Among all studied receptors, sorafenib exhibited its strongest predicted interaction with VEGFR-2, displaying a binding energy of −11.81 kcal/mol and forming four hydrogen bonds within the ATP-binding pocket. This observation is consistent with the known high affinity of sorafenib toward VEGFR-2 and supports its use as a reference ligand in this study.

Within the VEGFR2 protein pocket, Sorafenib demonstrates optimal positioning, with its core N-methylpicolinamide segment favorably located in the hinge region, and establishing hydrogen bonds of approximately 2.3 Å and 2.4 Å with amino acid residues. The 4-phenoxy substituent adopts an almost perpendicular orientation relative to the central scaffold, while the 4-chloro-3-trifluoromethylphenyl moiety reaches into the rear hydrophobic pocket. The urea linker further stabilizes the complex through three hydrogen bonds with Glu885 and Asp1046 at distances of 2.2 Å, 2.0 Å, and 1.9 Å, respectively (Wang *et al.,* 2024).

Analysis of the bis-urea derivatives demonstrated that each compound displayed a preferential binding profile toward specific kinases. Compounds 1a, 1e, and 1g showed their most favorable predicted binding energies with VEGFR-2, whereas compounds 1b and 1f exhibited stronger interactions with FGFR-1. Compound 1c showed its highest affinity toward BRAF, while compound 1d demonstrated preferential binding to FLT-3. These variations in binding behavior likely reflect differences in linker composition and spatial orientation of the bis-urea scaffold, which may influence accommodation within the ATP-binding pockets of distinct kinases (Chakraborty *et al.,* 2019). Compared with sorafenib, several derivatives exhibited comparable or lower predicted binding energies toward selected kinases, suggesting potentially favorable molecular interaction profiles. The detailed binding energies and hydrogen bond interactions are summarized in Table 1. Although docking results do not directly translate to biological activity, the observed interaction patterns provide insight into the potential multikinase inhibitory behavior of these derivatives and support further experimental evaluation. Visualized docking results of some ligands in complex with B-raf mutation receptors are shown in Figure 2.

3.2.2. ADME results for compounds 1a-g

The pharmacokinetic parameters of the compounds were assessed by QikProp and compared to those of sorafenib as the reference. The percentage of oral drug absorption for 1e (80.84%) and 1g (80.51%) was the highest among the derivatives, though still lower than sorafenib (94.94%).

Although compound 1e exhibited the highest lipophilicity (QPlogPo/w = 6.59), exceeding the Lipinski guideline threshold of 5, such elevated values are not uncommon among hydrophobic kinase inhibitors targeting specific enzyme pockets.

Table 1. Docking Results of Interactions between Sorafenib and its Derivatives with Approved Receptors as Potential Targets

		Sorafenib	**1a**	**1b**	**1c**	**1d**	**1e**	**1f**	**1g**
VEGFR2	BE	-11.81	-8.75	-8.6	-8.07	-6.95	-11.2	-8.2	-11.24
	H-b	4	4	4	0	2	1	1	2
	AA	Glu885* Cys919 Asp1046	Lys868 Arg1027 Asp1046 Leu1049	Lys868 Arg1027 Leu1049	-	Asp1046	Cys919	Glu885	Cys919 Asp1046
FGFR1	BE	-8.86	-7.33	-8.97	-7.44	-7.07	-10.37	-8.76	-9.45

	H-b	3	1	2	1	1	2	3	2
	AA	Phe642 Arg646 Arg622	Arg622	His621 Ala645	Asp527	Asp641	Ile620 Arg646	His621 Ala645 Asp652	Asp524 Asp647
BRAF	BE	-7.47	-6.34	-7.04	-7.58	-7.13	-8.07	-7.95	-9.82
	H-b	2	2	2	2	2	0	2	1
	AA	Ser465 Ser536	Ile617 Ser657	Asn580 Ile617	Ile613 Ser616	Cys532*	-	Gln494 Glu501	Ser536
RET	BE	-7.87	-7.13	-6.98	-4.96	-6.73	-7.16	-8.06	-9.75
	H-b	1	0	1	2	0	1	1	1
	AA	Ala807	-	Gly894	Leu779 Leu790	-	Lys780	Glu768	Arg770
KIT	BE	-6.99	-6.04	-6.91	-4.95	-5.09	-7.21	-7.51	-7.47
	H-b	3	1	3	3	2	2	2	2
	AA	Leu595* Asn819	Asp816	Lys581 Arg588 Gly610	Asp579 Ser645 Asn649	Arg634 Thr661	Asn649 Lys807	Tyr672 Asp816	Leu625 Arg634
FLT3	BE	-9.61	-6.64	-6.49	-7.82	-8.88	-7.75	-8.66	-9.73
	H-b	1	3	0	0	1	2	3	1
	AA	Cys828	Glu604 Leu677 Leu678	-	-	Glu692	Arg834 Ile836	Ser618 Cys694 Asp835	Glu661

Note. Active-site amino acids were identified based on reported crystallographic complexes from the Protein Data Bank (PDB) and literature data. BE, H-b, and AA mean Binding Energy, Hydrogen bond(s) formation, and Amino Acid, respectively. BE is based on kcal/mol. * Refers to the amino acids with more than one H-b with the ligand. The UniProt name of VEGFR2, FGFR1, BRAF, RET, KIT, and FLT3 includes Vascular Endothelial Growth Factor Receptor 2, Fibroblast Growth Factor Receptor 1, Serine/Threonine-protein kinase B-raf, Proto-oncogene Tyrosine-protein kinase receptor Ret, Mast/stem cell growth factor receptor Kit, and Receptor-type tyrosine-protein kinase FLT3, respectively.

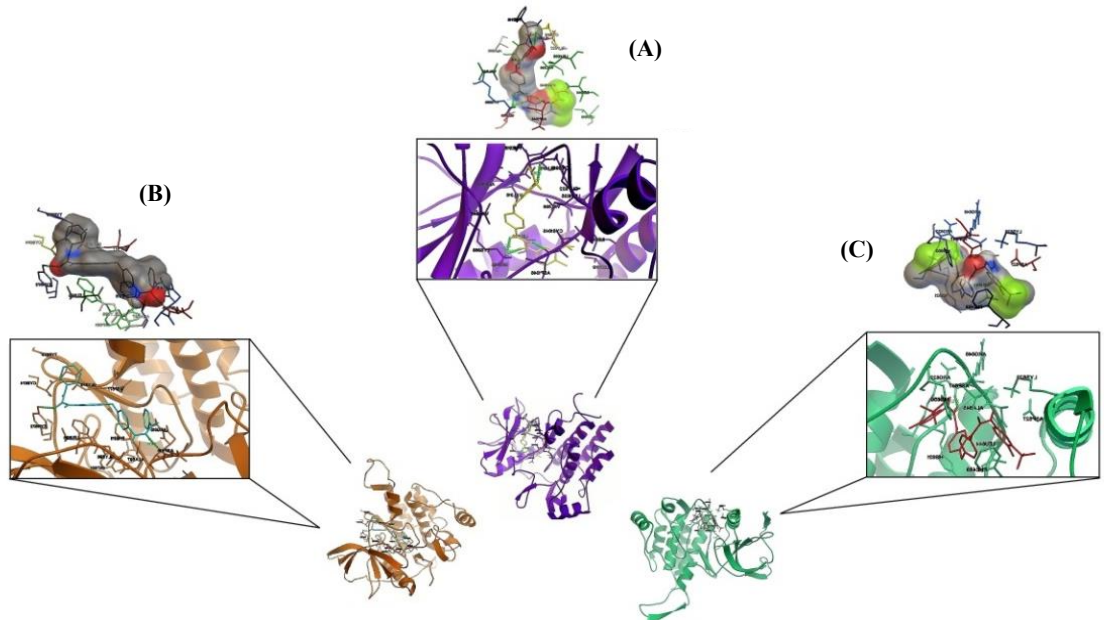

Figure 2. Docking results of three approved targets of sorafenib in complex with 1a-g candidate ligands and sorafenib: (A) Sorafenib in complex with VEGFR2, (B) 1f interactions with KIT, and (C) Complex of 1a with FGFR1 as receptor.

Increased lipophilicity may reduce aqueous solubility and potentially affect metabolic stability. Therefore, the drug-likeness of 1e should be interpreted with caution and validated experimentally.

Compound 1e also displayed a relatively low QPlogHERG value (−6.48), suggesting a potential risk of HERG channel inhibition. While in silico HERG predictions serve as useful early-stage alerts, they frequently overestimate cardiotoxicity for bulky kinase inhibitor scaffolds. Thus, this result warrants further investigation through experimental electrophysiological assays to accurately assess any potential cardiac safety concerns (Garrido *et al.,* 2020). The QPPCaco score (predicted Caco-2 cell permeability), which was used for computing the bowel-blood barrier, was good for all compounds (>25) except 1b (<25). The blood-brain barrier predictors (QPLogBB and QPPMDCK) were demonstrably strong; more specifically, QPLogBB for 1b, 1c, and 1e were similar to Sorafenib (-1), and the others were in the normal range (-3 to 1.2). Interestingly, QPPMDCK of 1a (2400.80), 1c (8978.21), and 1d (10000), 1e (10000) were definitely higher than Sorafenib (1683.62).

Regarding blood–brain barrier (BBB) related parameters, significant CNS penetration is generally not a primary requirement for systemic anticancer kinase

inhibitors, except in cases targeting primary or metastatic brain tumors. Therefore, the observed moderate to low QPlogBB values for most derivatives, and specifically the desirable range for compounds like 1b and 1f, are consistent with a pharmacokinetic profile that avoids extensive CNS exposure, thereby potentially minimizing off-target neurological effects.

QPlogKhsa (predicting parameter of binding to human serum albumin) scores for all compounds were in the acceptable range of -1.5 to 1.5. According to the QPlogHERG (IC_{50} value for blocking the HERG K^+ channels) for Sorafenib (-5.77), which is lower than -5 and so might be concerning, the 1g value of -5.64 might be acceptable, but the 1e value of -6.48 was lower than Sorafenib. However, the other compounds presented good scores for QPLogHERG. The QPLogKP (skin permeability) was outside the acceptable range for all compounds, including sorafenib, indicating poor dermal absorption.

Both Lipinski's Rule of Five and Jorgensen's Rule of Three were satisfied for all compounds, supporting their potential as drug-like molecules (≤5 and ≤3, respectively) (Table 2). In summary, compounds 1f, 1g, 1c, and 1d emerge as the most promising candidates from this in silico ADME assessment for further experimental investigation.

3.2.3. Antioxidant Assay

The colorimetric DPPH method was used to evaluate the antioxidant activity of the compounds. The DPPH assay was included to explore the antioxidant potential of the bis-urea scaffold as an auxiliary physicochemical property, rather than a mechanism directly related to kinase inhibition. DPPH or 2,2-diphenyl-2-picrylhydrazyl is a free radical with high stability that can receive a hydrogen radical or an electron to produce a stable molecule. DPPH shows a strong absorption band at 517 nm, which decreases upon electron acceptance, leading to a color change from purple to colorless (Bondet *et al.,* 1997).

The decrease in the absorption band depends on the antioxidant ability of compounds. A greater decrease in absorption bands results from the higher antioxidant activity of the compounds. Radical scavenging activity of compounds 1a–g was measured at concentrations ranging from 62.5 to 2000 µg/mL in MeOH. IC_{50} values were measured by plotting radical scavenging activity against concentration and determining the concentration required to scavenge 50% of the DPPH radicals. Ascorbic acid was used as the standard, and analyses were completed in triplicate.

Table 2. Pharmacokinetic Parameters of Compounds 1a-g Compared with Sorafenib

Compound	QPLogPo/w[a]	QPLogHERG[b]	QPPCaco[c]	QPLogBB[d]	QPPMDCK[e]	QP LogKP[f]	QPLogKhsa[g]	Human Oral Absorption[h]	Lipinski's Rule of Five	Jorgensen's Rule of Three
Acceptable Range	(-2.0 to 6.5)	>-5	<25 is poor, >500 is great	(-3 to 1.2)	<25 is poor, >500 is great	(-8.0 to -1)	(-1.5 to 1.5)	<25% is low, 80%> is High	≤4	≤3
1a	5.53	-2.43	30.52	0.81	2400.80	-3.39	0.85	59.99	2	0
1b	3.57	-1.64	13.86	-1	717	-4.19	0.23	55.34	1	1
1c	5.75	-3.88	92.04	-1	8978.21	-2.79	0.65	69.83	2	1
1d	4.55	-3.67	115.95	-0.57	10000	-2.98	0.25	77.58	1	1
1e	6.59	-6.48	199.73	-1	10000	-2.18	0.98	80.84	2	1
1f	2.78	-2.06	38.88	-1.2	94.24	-2.79	0.06	71.68	0	0
1g	3.53	-5.64	68.44	-1.95	106.19	-1.85	0.14	80.51	0	0
Sorafenib	4.15	-5.77	275.14	-1	1683.62	-2.47	0.35	94.94	0	1

Note. The ADME parameters predict by Qiqprop. a refers to as Predicted octanol/water partition coefficient, b means Predicted IC_{50} value for blocking the HERG K^+ Channels, c scores the Predicted apparent Caco-2 cell permeability in nm/sec, d refers to Predicted brain/blood partition coefficient, e is Predicted apparent MDCK cell permeability in nm/sec, f means Predicted skin permeability, log Kp, g predicts the binding to human serum albumin, and h measures human oral absorption in the range of 0 to 100%.

Among the tested derivatives, only compounds 1e and 1f exhibited measurable radical scavenging activity within the tested concentration range; therefore, only these compounds were further analyzed and reported. Along with Figure 3, radical scavenging activity improved with concentration. As a result of the extended conjugated system, which improves resonance and stabilizes free radicals, compound 1e exhibited the highest DPPH radical scavenging activity. The IC_{50} values of compounds are presented in Table 3.

Table 3. IC_{50} Values by DPPH Assay of Compounds 1e and 1f and Comparison to Ascorbic Acid

Compound	DPPH assay IC_{50} (µm)
1e	5.35
1f	14.28
Ascorbic Acid	6.00

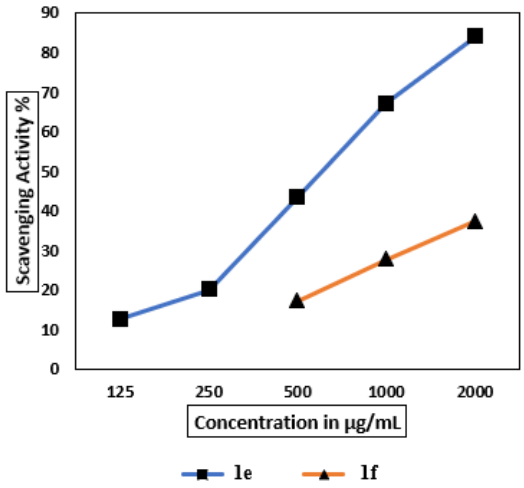

Figure 3. DPPH radical scavenging activity of compounds 1e and 1f.

4. Conclusion

In conclusion, seven previously synthesized bis-urea derivatives featuring diverse linker moieties (1a-g) inspired by the sorafenib framework were evaluated using molecular docking, in silico pharmacokinetic analyses, and antioxidant assays. Overall, the in silico pharmacokinetic and docking analyses suggest that certain bis-urea derivatives may show promising molecular interaction patterns and suitable drug-likeness properties. These findings provide a computational basis for future experimental investigations, rather than definitive evidence of superior biological activity.

The antioxidant potential of the compounds was assessed using the DPPH assay, with derivatives 1e and 1f showing notable radical-scavenging activity compared to ascorbic acid. Future studies will include comprehensive experimental validation to better define the pharmacological relevance of these bis‑urea derivatives. This will involve kinase inhibition assays against key targets associated with the sorafenib framework, as well as broader cytotoxicity profiling to evaluate their biological impact in cellular models. Additionally, incorporating advanced computational approaches, including molecular dynamics simulations and QSAR modeling, will also support a more refined understanding of structure–activity relationships.

Conflict of interest

The authors declare no conflict of interest.

Acknowledgment

The authors are grateful to the Research Council of the University of Guilan for financial support of this research work.

Ethical approval

This article does not contain any studies with human participants or animals performed by any of the authors.

Funding

None declared.

Authors' Contributions

Sajede Shoja: Design of the work, Conceptualization, Docking simulation, Acquisition, Interpretation of data, Data curation and Validation, Writing-original draft, Review and editing; Elham Gholibegloo: Acquisition, Data curation and Validation, Review and editing; Nosrat O (Allah) Mahmoodi: Conceptualization, supervision, data interpretation, review and editing, and final approval version to be published. All authors have read and approved the final version of the manuscript.

References

Aliabadi, R. S., Mahmoodi, N. O., Ghafoori, H., Roohi, H., & Pourghasem, V. (2018). Design and synthesis of novel bis-hydroxychalcones with consideration of their biological activities. *Research on Chemical Intermediates*, *44*(5), 2999-3015.

Bondet, V., Brand-Williams, W., & Berset, C. (1997). Kinetics and mechanisms of antioxidant activity using the DPPH. free radical method. *LWT-Food Science and Technology*, *30*(6), 609-615.

Chakraborty, S., Inukai, T., Fang, L., Golkowski, M., & Maly, D. J. (2019). Targeting Dynamic ATP-Binding Site Features Allows Discrimination between Highly Homologous Protein Kinases. *ACS Chem Biol*, *14*(6), 1249-1259. https://doi.org/10.1021/acschembio.9b00214

Davies, H., Bignell, G. R., Cox, C., Stephens, P., Edkins, S., Clegg, S., Teague, J., Woffendin, H., Garnett, M. J., & Bottomley, W. (2002). Mutations of the BRAF gene in human cancer. *Nature*, *417*(6892), 949-954.

Dumaz, N., & Marais, R. (2003). Protein kinase A blocks Raf-1 activity by stimulating 14-3-3 binding and blocking Raf-1 interaction with Ras. *Journal of Biological Chemistry*, *278*(32), 29819-29823.

Garrido, A., Lepailleur, A., Mignani, S. M., Dallemagne, P., & Rochais, C. (2020). hERG toxicity assessment: Useful guidelines for drug design. *European Journal of Medicinal Chemistry*, *195*, 112290. https://doi.org/10.1016/j.ejmech.2020.112290

Guan, A., Liu, C., Yang, X., & Dekeyser, M. (2014). Application of the intermediate derivatization approach in agrochemical discovery. *Chem Rev*, *114*(14), 7079-7107. https://doi.org/10.1021/cr4005605

Guex, N., & Peitsch, M. C. (1997). SWISS-MODEL and the Swiss-Pdb Viewer: an environment for comparative protein modeling. *electrophoresis*, *18*(15), 2714-2723.

Holderfield, M., Merritt, H., Chan, J., Wallroth, M., Tandeske, L., Zhai, H., Tellew, J., Hardy, S., Hekmat-Nejad, M., & Stuart, D. D. (2013). RAF inhibitors activate the MAPK pathway by relieving inhibitory autophosphorylation. *Cancer cell*, *23*(5), 594-602. https://www.drugbank.ca/drugs/DB00398.

Jin, L., Zhang, Y., Yan, L., Guo, Y., & Niu, L. (2012). Phenolic compounds and antioxidant activity of bulb extracts of six Lilium species native to China. *Molecules*, *17*(8), 9361-9378.

Jorgensen, W. L., & Duffy, E. M. (2000). Prediction of drug solubility from Monte Carlo simulations. *Bioorganic & medicinal chemistry letters*, *10*(11), 1155-1158.

Lemmon, M. A., & Schlessinger, J. (2010). Cell signaling by receptor tyrosine kinases. *Cell*, *141*(7), 1117-1134. https://doi.org/10.1016/j.cell.2010.06.011

Li, Q., Li, T., Woods, K. W., Gu, W. Z., Cohen, J., Stoll, V. S., Galicia, T., Hutchins, C., Frost, D., Rosenberg, S. H., & Sham, H. L. (2005). Benzimidazolones and indoles as non-thiol farnesyltransferase inhibitors based on tipifarnib scaffold: synthesis and activity. *Bioorg Med Chem Lett*, *15*(11), 2918-2922. https://doi.org/10.1016/j.bmcl.2005.03.049

Liao, J. J.-L. (2007). Molecular Recognition of Protein Kinase Binding Pockets for Design of Potent and Selective Kinase Inhibitors. *Journal of Medicinal Chemistry*, *50*(3), 409-424. https://doi.org/10.1021/jm0608107

Lim, W. K., Rösgen, J., & Englander, S. W. (2009). Urea, but not guanidinium, destabilizes proteins by forming hydrogen bonds to the peptide group. *Proc Natl Acad Sci U S A*, *106*(8), 2595-2600. https://doi.org/10.1073/pnas.0812588106

Lipinski, C. A., Lombardo, F., Dominy, B. W., & Feeney, P. J. (2012). Experimental and computational approaches to estimate solubility and permeability in drug discovery and development settings. *Advanced drug delivery reviews*, *64*, 4-17.

Lovell, S. C., Davis, I. W., Arendall III, W. B., De Bakker, P. I., Word, J. M., Prisant, M. G., Richardson, J. S., & Richardson, D. C. (2003). Structure validation by Cα geometry: ϕ, ψ and Cβ deviation. *Proteins: Structure, Function, and Bioinformatics*, *50*(3), 437-450.

Mahmoodi, N. O., Khalili, B., Rezaeianzade, O., & Ghavidast, A. (2016). One-pot multicomponent synthesis of indol-3-yl-hydrazinyl thiazoles as antimicrobial agents. *Research on Chemical Intermediates*, *42*(8), 6531-6542.

Mahmoodi, N. O., Namroudi, M., Ghanbari Pirbasti, F., Roohi, H., & Nikokar, I. (2016). Practical one-pot synthesis of semicarbazone derivatives via semicarbazide, and evaluation of their antibacterial activity. *Research on Chemical Intermediates*, *42*(4), 3625-3636.

Mahmoodi, N. O., Shoja, S., Sharifzadeh, B., & Rassa, M. (2014). Regioselective synthesis and antibacterial evaluation of novel bis-pyrimidine derivatives via a three-component reaction. *Medicinal Chemistry Research*, *23*(3), 1207-1213.

Mahmoodi, N. O., Shoja, S., Tabatabaeian, K., & Sharifzadeh, B. (2015). Ultrasound-promoted one-pot five-components synthesis of biologically active novel bis ((6-alkyl or phenyl-2-phenylpyrimidine-4-yl) oxy) alkane or methyl benzene derivatives. *Ultrasonics Sonochemistry*, *23*, 31-36.

Morris, G. M., Huey, R., Lindstrom, W., Sanner, M. F., Belew, R. K., Goodsell, D. S., & Olson, A. J. (2009). AutoDock4 and AutoDockTools4: Automated docking with selective receptor flexibility. *Journal of computational chemistry*, *30*(16), 2785-2791. https://doi.org/10.1002/jcc.21256

Nazarian, R., Shi, H., Wang, Q., Kong, X., Koya, R. C., Lee, H., Chen, Z., Lee, M.-K., Attar, N., & Sazegar, H. (2010). Melanomas acquire resistance to B-RAF (V600E) inhibition by RTK or N-RAS upregulation. *Nature*, *468*(7326), 973-977.

Nexavar® (Sorafenib) Scientific Discussion EMEA WC500027707. (2007).

QikProp, Schrödinger, LLC, New York, NY, 2018. . (2018).

Shoja, S., Mahmoodi, N. O., Ghafouri, H., Rassa, M., Sharafshah, A., & Panahi Kokhdan, E. (2020). Design, in silico, one-pot synthesis, and biological evaluations of novel bis-urea analogs. *Research on Chemical Intermediates*, *46*(7), 3327-3339.

Sippl, M. J. (1993). Recognition of errors in three-dimensional structures of proteins. *Proteins: Structure, Function, and Bioinformatics*, *17*(4), 355-362.

Sorafenib, BAY43-9006 (Nexavar®, Bayer) NDA 21923 Medical Review (2005). FDA Retrieved from https://www.accessdata.fda.gov/drugsatfda_docs/nda/2005/021923_s000_Nexavar_MedR.pdf

Stumpe, M. C., & Grubmüller, H. (2007). Interaction of Urea with Amino Acids: Implications for Urea-Induced Protein Denaturation. *Journal of the American Chemical Society*, *129*(51), 16126-16131. https://doi.org/10.1021/ja076216j

Terefenko, E. A., Kern, J., Fensome, A., Wrobel, J., Zhu, Y., Cohen, J., Winneker, R., Zhang, Z., & Zhang, P. (2005). SAR studies of 6-aryl-1,3-dihydrobenzimidazol-2-ones as progesterone receptor antagonists. *Bioorg Med Chem Lett*, *15*(15), 3600-3603. https://doi.org/10.1016/j.bmcl.2005.05.082

Wang, Z., Sun, L., Xu, Y., Huang, J., Yang, F., & Chang, Y. (2024). Discovery of novel VEGFR2 inhibitors against non-small cell lung cancer based on fingerprint-enhanced graph attention convolutional network. *J Transl Med*, *22*(1), 1097. https://doi.org/10.1186/s12967-024-05893-2

Wiederstein, M., & Sippl, M. J. (2007). ProSA-web: interactive web service for the recognition of errors in three-dimensional structures of proteins. *Nucleic acids research*, *35*(suppl_2), W407-W410.

Wilhelm, S. M., Adnane, L., Newell, P., Villanueva, A., Llovet, J. M., & Lynch, M. (2008). Preclinical overview of sorafenib, a multikinase inhibitor that targets both Raf and VEGF and PDGF receptor tyrosine kinase signaling. *Molecular cancer therapeutics*, *7*(10), 3129-3140.

Winum, J.-Y., Maresca, A., Carta, F., Scozzafava, A., & Supuran, C. T. (2012). Polypharmacology of sulfonamides: pazopanib, a multitargeted receptor tyrosine kinase inhibitor in clinical use, potently inhibits several mammalian carbonic anhydrases. *Chemical Communications*, *48*(66), 8177-8179.

Yuen, S. T., Davies, H., Chan, T. L., Ho, J. W., Bignell, G. R., Cox, C., Stephens, P., Edkins, S., Tsui, W. W., & Chan, A. S. (2002). Similarity of the phenotypic patterns associated with BRAF and KRAS mutations in colorectal neoplasia. *Cancer research*, *62*(22), 6451-6455.

Zhang, Y., Chen, Y., Zhang, D., Wang, L., Lu, T., & Jiao, Y. (2018). Discovery of Novel Potent VEGFR-2 Inhibitors Exerting Significant Antiproliferative Activity against Cancer Cell Lines. *J Med Chem*, *61*(1), 140-157. https://doi.org/10.1021/acs.jmedchem.7b01091

How to cite this paper:

Shoja, S., Gholibegloo, E. & Mahmoodi, N. (2026). *In Silico* Pharmacokinetic Profiling, Molecular Docking, and Antioxidant Assessment of Bis-Urea Derivatives Derived from the Sorafenib Scaffold. *Microbiology, Metabolites and Biotechnology, 6*(2), xx-xx..
DOI: 10.22104/mmb.2026.8141.1198